


 Cite this: *RSC Adv.*, 2025, **15**, 20200

## ***Croton bonplandianus* leaves extract to mitigate the hazardous effect of *Meloidogyne incognita*: GC-MS and molecular docking analysis of nematicidal compounds**

Ahmed Hussain Jawhari, <sup>a</sup> Faris Alfifi, <sup>a</sup> Abdullah Ali Alamri, <sup>ab</sup> Islam Mazahirul <sup>c</sup> and Syed Kashif Ali <sup>\*ab</sup>

Active metabolites from plants are considered safer than synthetic chemicals for the control of plant-parasitic nematodes. *Meloidogyne incognita*, one of the most detrimental plant-parasitic nematodes, causes considerable agricultural losses and reductions in yield globally. Commonly used chemical nematicides have been withdrawn due to growing environmental and human health concerns. The need for alternate nematode management techniques is fueled by the enormous demand for environmentally acceptable bio-nematicides that have advantageous qualities for plants. Using *in vitro* tests, the current study aimed to ascertain the nematicidal potential of different concentrations of *Croton bonplandianus* leaf extract-200, 400, 600, and 800 ppm against *M. incognita*. According to our findings, J2s mortality and egg hatching inhibition varied in degree across all investigated dosages. We detected 24 chemicals using GC-MS, with 4-vinylphenol, *n*-hexadecanoic acid, delta-tocopherol, gamma sitosterol and others being the main ones. The nematicidal possibilities of *C. bonplandianus* were further substantiated using *in silico* molecular docking, which examined the binding affinities of its principal constituents, 4-vinylphenol and gamma-sitosterol, with the odorant response gene 1 (ODR 1) protein of *M. incognita*. The present investigation emphasizes the significance of strategic biomolecule selection and examines the biochemical interactions between ligands and target proteins, providing helpful insights for subsequent studies. Therefore, to manage root-knot nematodes and lower environmental concerns, plant extract containing nano bio-molecules might be the ideal substitute for chemical nematicides.

Received 8th February 2025  
 Accepted 24th April 2025

DOI: 10.1039/d5ra00931f  
[rsc.li/rsc-advances](http://rsc.li/rsc-advances)

### 1. Introduction

The consequences of climate change are causing rapid environmental changes throughout the world. The prevalence and severity of plant diseases are rising across many locations and crops globally, which is one of the main effects of rising global temperatures. The spread and severity of plant-parasitic nematodes (PPNs), which have increased in frequency as a result of changing environmental circumstances, have been greatly impacted by climate change, among other ecological interactions.<sup>1</sup> In addition to having an impact on plant health, these climate changes also reduce agricultural productivity, which results in large financial losses. Because of their capacity to seriously harm plant roots, which ultimately impacts the host

plant's entire vascular system, root-knot nematodes (RKNs) of the genus *Meloidogyne* have become a severely debilitating infection among these plant-parasitic nematodes. Modern farming methods have developed to ensure sustainable agricultural operations and lessen the negative consequences of climate change. Protective agriculture is one such strategy, which aims to increase output while preserving water and land resources and minimizing environmental damage.<sup>2</sup> The goal of protective agriculture is to minimize external risks, such as pests and diseases, while simultaneously establishing ideal growing conditions for plants. RKNs, however, remain a serious threat to global food security despite improvements in farming practices. Because of their high degree of adaptability, these worms can infect a variety of plant species, resulting in substantial root damage, reduced growth, and decreased production.

Among the most damaging PPNs (*Meloidogyne* spp.), have a major effect on crop productivity worldwide. Their active parasitism causes distinctive root galls to grow, which interfere with the plant's vascular system and make it more difficult for nutrients and water to be transported effectively. Consequently,

<sup>a</sup>Department of Physical Sciences, Chemistry Division, College of Science, Jazan University, P.O. Box. 114, Jazan 45142, Kingdom of Saudi Arabia. E-mail: [skali@jazanu.edu.sa](mailto:skali@jazanu.edu.sa)

<sup>b</sup>Nanotechnology Research Unit, Jazan University, P.O. Box 114, Jazan 45142, Kingdom of Saudi Arabia

<sup>c</sup>Department of Biology, College of Science, Jazan University, PO Box No 114, Jazan 45142, Kingdom of Saudi Arabia



signs including chlorosis, wilting, and stunted development are displayed by the diseased plants, which eventually lowers agricultural productivity.<sup>3</sup> Due to their wide host range and ability to flourish in a variety of environmental settings, RKN infestations result in significant economic losses. Their harm goes beyond simple crop losses; they also make plants more vulnerable to secondary bacterial, fungal, and viral illnesses, which make managing pests much more difficult.<sup>4</sup> It is predicted that PPNs, especially RKNs, cause 8.8–14% of crop losses globally each year, with an annual impact of about USD 173 billion.<sup>5</sup> These startling losses show how urgently sustainable nematode control methods are needed to ensure food security.

Since chemical nematicides have been successful in lowering nematode populations, they have been the mainstay of RKN management for many years. However, there are significant worries about environmental contamination, dangers to human health, and the emergence of nematode resistance due to their widespread use.<sup>6</sup> Numerous chemical nematodes are extremely harmful to organisms that are not their intended targets, which leads to soil deterioration and water contamination. Furthermore, small-scale farmers cannot afford them, which exacerbate the problems with food security in areas with low resources. As a result, the hunt for safer and more environmentally friendly substitutes has accelerated considerably. As viable substitutes for chemical nematicides, botanical extracts and bio-based nematicides provide efficient management with reduced environmental hazards.<sup>7</sup> Numerous bioactive secondary metabolites that have potent nematicidal effects are produced by plants, such as alkaloids, flavonoids, tannins, terpenoids, steroids, and phenols.<sup>7–9</sup> These substances decrease RKN populations, interfere with reproduction, and disturb nematode life cycles. Numerous plant extracts have shown notable nematicidal activity and benefits for soil health, including those made from sesame stalk, neem cake, crab shell meal, quillaja, and tannins.<sup>10–12</sup> *In vitro* and pot tests have shown that certain plant-derived chemicals, such as aldehydes like furfural from *Melia azedarach* and (E,E)-2,4-decadienal from *Ailanthus altissima*, as well as ketones like 2-undecanone from *Ruta chalepensis*, are very efficient against RKNs.<sup>13,14</sup>

Advanced analytical methods like molecular docking and gas chromatography-mass spectrometry (GC-MS) are frequently used to further improve the development of plant-based nematicides. Effective nematicidal drugs can be found more easily thanks to GC-MS's ability to identify and characterize bioactive chemicals in plant extracts.<sup>15,16</sup> The design of strong and specific nematodes is aided by molecular docking, which sheds light on the binding interactions between plant phytochemicals and nematode target proteins.<sup>17–19</sup> An effective method for managing RKN sustainably is the incorporation of nematicides generated from plants into agricultural operations. These environmentally friendly substitutes help to increase soil health, biodiversity, and long-term agricultural viability by lowering dependency on chemical nematicides. This study demonstrates how *M. incognita* can be controlled to lessen its detrimental effects on a variety of commercially important crops by using an extract from *C. bonplandianus* leaves. Additionally, it looks at possible mechanisms for controlling *M.*

*incognita* based on *in silico* molecular docking study and GC-MS analysis to identify active phyto-compounds in *C. bonplandianus* leaf extract.

## 2. Materials and methods

### 2.1 Collection and multiplication of *M. incognita* inoculum (J2s)

Infected brinjal roots with *Meloidogyne* spp. were gathered from Wadi Khulab in the Jizan region, Saudi Arabia. The species *M. incognita* was identified using perineal pattern morphology, adhering to the methods established by Eisenback and Hunt.<sup>20</sup> The nematodes were later cultivated on brinjal plants in a controlled greenhouse at the Department of Biology, Jazan University, Jazan, Saudi Arabia. In order to acquire an adequate number of *M. incognita* second-stage juveniles (J2s), infected brinjal plants were meticulously uprooted, guaranteeing the retention of egg masses on the roots. The roots were meticulously rinsed with distilled water to eliminate attached soil particles. Egg masses were delicately removed from the roots using sterile forceps, cleaned with double-distilled water (DDW), and positioned on 25 µm pore-size mesh sieves lined with tissue paper. The sieves were placed in Petri dishes containing a suitable volume of water to promote egg hatching. The Petri plates were incubated in a BOD chamber to facilitate the hatching of J2s. Upon emergence, the juveniles traversed the mesh and settled at the base of the Petri dishes, whilst the egg masses remained on the sieve. Fresh deionized distilled water was consistently supplied, and the J2 suspension was collected daily. The concentration of newly hatched J2s was calibrated as required and preserved for future research.

### 2.2 Collection and extraction of *C. bonplandianus* leaf extract

The Wadi Khulab, Jizan, in Saudi Arabia, is where the fresh *C. bonplandianus* leaves were gathered. After that, the leaves were left to cool in an open area. For four weeks, they were let to dry naturally. A mortar and pestle were used to grind the leaves finely when they had completely dried. About 0.5 g of powdered leaves and 20 mL of HPLC-grade methanol were combined to create the extract. After vortexing and 15 minutes of ultrasonic treatment, the mixture was centrifuged for 15 minutes at 500 rpm. The extract was filtered with Whatman filter paper No. 1 and then analyzed with GC-MS. For additional testing, a purified solution was created by dissolving 1.0 g of desiccated *C. bonplandianus* leaves powdered in 1000 mL of DDW. The fluid was subsequently filtered using a Whatman filter and employed for hatching and mortality experiments.

### 2.3 GC-MS testing of leaf extract of *C. bonplandianus*

The bioactive components in the methanolic leaf extracts were detected utilizing a Shimadzu QP2010 Plus GC-MS system fitted with a Rtx-5MS capillary column (30 m in length and 0.25 mm in diameter). Helium served as the carrier gas, and a 1 µL sample volume was injected into the column at a flow rate of 1.21 mL per minute. The oven temperature was initially set at 100 °C,



then incrementally raised at a rate of 5 °C per minute until it attained 250 °C, followed by an additional rise of 10 °C per minute to a final temperature of 280 °C. Metabolite profiling was performed utilizing a mass spectrometry (MS) detector in full scan mode, facilitating the identification of unique peak fragmentation patterns associated with different metabolites. The acquired raw data were analyzed using GC-MS Solutions software (Lab Solutions), enabling chromatographic analysis, peak identification, and manual integration of pertinent peaks for thorough metabolite characterization. The software also made it possible to deconstruct complicated chromatograms in order to identify overlapping signals, which increased the precision of metabolite detection. The main way that metabolites were identified was by their retention times, which are important for describing different molecules in the sample matrix.

Additionally, by analyzing molecular masses and merging the distinct peak regions that correspond to each component, the quantification of discovered metabolites was accomplished. The peak spectra that were produced were compared in a methodical manner with reference mass spectra that were taken from three well-known spectrum databases. This was done in order to guarantee that the identification was accurate. The National Institute of Standards and Technology (NIST 14), the NIST 14 s, and the Wiley 8 database were the databases that were being taken into consideration. By reducing incorrect identifications, this comparative method greatly increased the confidence in compound annotation. Internal standards were also used as a quality control measure, guaranteeing repeatability across analytical runs and validating metabolite detection. A strong analytical framework for accurate metabolite identification and quantification was produced by combining spectrum matching, retention time correlation, and internal standard comparison.

#### 2.4 Hatching bioassay

The inhibitory effect of *C. bonplandianus* leaf extract at different concentrations (200, 400, 600, and 800 ppm) on the hatching of *M. incognita* J2 was evaluated using the egg mass dipping method. Fresh egg masses were meticulously selected from the galled roots of brinjal plants, followed by the removal of debris through three or four rinses with deionized distilled water. Six newly collected egg masses were placed in Petri dishes containing 10 mL of leaf extract at varying concentrations, following standard protocols. Each Petri dish was sealed with parafilm and maintained in an incubator at a constant temperature of 28 °C to prevent evaporation. Egg masses immersed in DDW served as the control group. To ensure reliability, each treatment, excluding the control, was replicated six times. The experiment was conducted twice to verify the accuracy of the findings. Following a four-day incubation period, the total number of hatched J2s from the egg masses in each replicate was quantified using a binocular microscope. The provided formula was utilized to calculate the percentage inhibition of J2 hatching based on the mean data.<sup>21</sup>

$$\text{Percent hatching inhibition} = \left( \frac{C_0 - T_\alpha}{C_0} \right) \times 100$$

where  $C_0$  = number of hatched J2s in DDW (control).  $T_\alpha$  = number of hatched J2s in each concentration of *C. bonplandianus* leaf extract.

#### 2.5 Mortality bioassay

In Petri plates, 1 mL of nematode suspension containing 70 J2s was added to 9 mL of *C. bonplandianus* leaf extract at concentrations of 200, 400, 600, and 800 ppm to assess the anti-nematode effects on J2s of *M. incognita*. Petri dishes containing DDW served as the control. Petri dishes were sealed with parafilm and incubated at 28 °C for a specified duration to minimize drying. After exposure intervals of 12, 24, 48, and 72 hours, the counts of live and dead J2s were conducted using a binocular microscope. According to El-Rokiek and El-Nagdi,<sup>22</sup> second stage juveniles exhibiting movement or a snaky shape were classified as alive, whereas J2s that displayed no movement and had a straight body shape were classified as dead.<sup>23</sup> The experiment utilized six duplicates for each concentration, and LC50 values were determined.<sup>24,25</sup> The study was conducted on two separate occasions to validate the findings. The following formula was employed to calculate the percentage mortality of second stage juveniles:

$$\text{Percent mortality of J2s} = \left( \frac{\text{Total J2s} - \text{Dead J2s}}{\text{Total J2s}} \right) \times 100$$

#### 2.6 Molecular modeling and docking

AutoDock 4.2 was utilized to conduct a molecular docking analysis to assess the interaction between Odorant Response Gene 1 (ODR 1) and the ligands 4-vinylphenol and gamma-sitosterol. The three-dimensional structure of ODR 1 (PDB ID: 3K1E) was sourced from the RCSB Protein Data Bank and underwent preprocessing, which involved the removal of water molecules and redundant heteroatoms, the addition of polar hydrogens, and the assignment of Gasteiger charges. The final processed structure was transformed into PDBQT format for docking purposes. The molecular structures of 4-vinylphenol (CID: 62453) and gamma-sitosterol (CID: 457801) were obtained from PubChem. Prior to docking, the ligands underwent optimization utilizing the MMFF94 force field for energy minimization, with rotatable bonds identified to improve flexibility. Furthermore, Gasteiger charges were assigned, and the ligands were transformed into PDBQT format.<sup>26–29</sup>

The docking grid was set to 120 × 120 × 120 points, with a spacing of 0.375 Å, to align with the ODR 1 binding site and facilitate a thorough search for interactions. The Lamarckian Genetic Algorithm (LGA) was utilized for docking simulations, involving 100 independent runs. The docking parameters comprised 2 500 000 energy evaluations, a population size of 150, a crossover rate of 0.8, and a mutation rate of 0.02. The conformations were ranked according to binding energy, and the most stable configurations were selected for further



analysis. Binding energy, hydrogen bonds, and hydrophobic interactions were analyzed through visualization and interaction studies conducted with Discovery Studio Visualizer and PyMOL. The identification of critical residues involved in ligand binding provided enhanced understanding of the molecular interactions between ODR 1 and the ligands under investigation. This study elucidates the binding affinity and interaction dynamics of 4-vinylphenol and gamma-sitosterol with ODR 1.

### 2.7 Statistical analysis

The statistical analysis of the collected data across various studied variables was performed using R software (version 2.14.1). Duncan's multiple range test (DMRT) was utilized to determine significant differences ( $p = 0.05$ ) among the assessed attributes. ANOVA was conducted utilizing OPSTAT.<sup>30</sup> Furthermore, OPSTAT was employed to ascertain the LC<sub>50</sub> values for each treatment.<sup>30</sup>

## 3. Results and discussion

### 3.1 Hatching

The effect of varying leaf extract concentrations (200, 400, 600, and 800 ppm) on the suppression of J2 hatching was assessed in this bioassay using a direct contact approach. Across the investigated concentrations, a notable variance in inhibition was noted (Fig. 1). All concentrations of the extract significantly decreased J2 hatching as compared to the control (DDW). Both the treatment's efficacy and the reduction of J2 hatching increased with the extract concentration. In contrast to the control, hatching was significantly reduced at even the lowest concentration (200 ppm). After a 4 days incubation period, the maximum suppression was observed at 800 ppm, followed by 600 ppm and 400 ppm. The inhibitory effect on J2 hatching gradually rose from 200 ppm to 800 ppm. The 200 ppm had the least effect on J2 hatch inhibition of any concentration

examined. Fig. 1 shows the distinct inhibitory effects of various extract concentrations on J2 hatching.

### 3.2 Mortality

The fluctuation in the rate of J2s death in the extract's aqueous concentration at various incubation times is displayed in Table 1 and Fig. 2. In water (control), we found that J2s mortality was zero. The parallel study found that the J2s mortality rate was lowest at 200 ppm and highest at 800 ppm during a 72 hours incubation period. The observed pattern of J2s death was directly correlated with the incubation time and concentration strength. The extract was shown to be somewhat detrimental to *M. incognita* J2s at all tested concentrations, with J2s mortality at 72 hours of exposure ranging from 13% to 81% (Table 1). After 72 hours of incubation, the 800 ppm extract was shown to be highly deadly to J2s. Generally speaking, J2s' mortality rose as the incubation time and concentration increased. Following immersion in extract, the LC<sub>50</sub> value for mortality in J2s was calculated at four distinct exposure times: 12, 24, 48, and 72 hours. For J2s mortality, the extract's LC<sub>50</sub> values at 12, 24, 48, and 72 hours of exposure period were 1982.43, 834.64, 468.46, 299.55 ppm, respectively. According to this data, the LC<sub>50</sub> value was higher for killing half of the J2s population during the brief exposure period; however it was lower for a prolonged exposure period. As incubation time increases, the treatment's LC<sub>50</sub> value drops, indicating that treatments with high LC<sub>50</sub> values were less harmful to *M. incognita* J2s (Table 2).

Using plant extracts to manage RKNs is a sustainable and environmentally benign alternative to chemical nematodes, which often have detrimental ecological repercussions. Plant-derived extracts encourage environmental sustainability because they are biodegradable and present few hazards to non-target creatures, in contrast to synthetic pesticides. However several issues must be resolved, such as cost-effectiveness. Seasonal plant material availability and extraction and

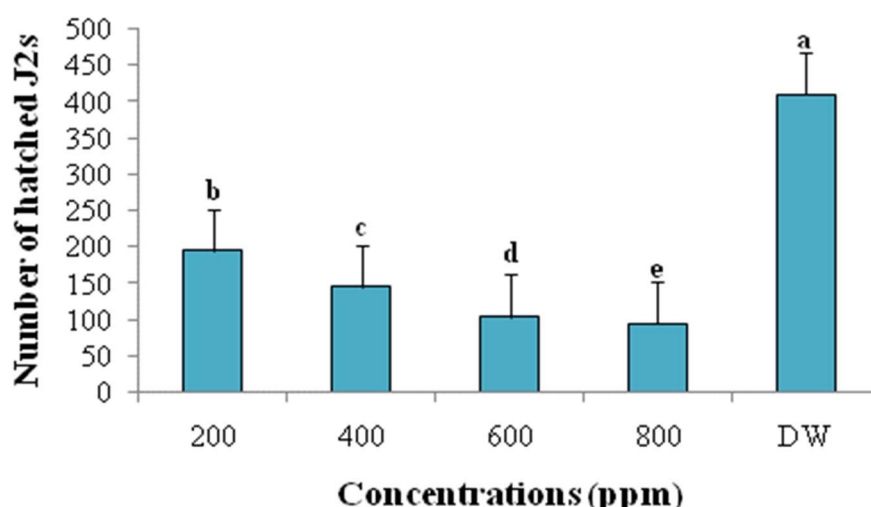


Fig. 1 Effect of several concentrations of *C. bonplandianus* leaves extract on J2s hatching of *M. incognita* over 5 days of incubation period under *in vitro*. Each value is an average of six replicate. Each bar followed by same letter is not significantly different according to Duncan's multiple-range test ( $p \leq 0.05$ ). [DW-distilled water (Control); J2s-second stage juveniles; ppm-parts per million].



**Table 1** Effect of different concentrations of *C. bonplandianus* leaves extract on the mortality of J2s of *M. incognita* over 12, 24, 48 and 72 hours of incubation under *in vitro*<sup>a</sup>

Treatment	Concentrations (ppm)	Number of dead J2s (mean $\pm$ SE) at different time intervals (hours)			
		12	24	48	72
<i>C. bonplandianus</i> leaves extract	200	10d $\pm$ 1 (13%)	16d $\pm$ 1.54 (21.33%)	23d $\pm$ 1.52 (30.66%)	30d $\pm$ 1.73 (40%)
	400	15c $\pm$ 1.15 (20%)	24c $\pm$ 1.54 (32%)	32c $\pm$ 1.52 (42.66%)	42c $\pm$ 1.73 (56%)
	600	19b $\pm$ 1.52 (25.33%)	31b $\pm$ 1.52 (41.33%)	40b $\pm$ 1.73 (53.33%)	50b $\pm$ 2.08 (66.66%)
	800	26a $\pm$ 2.08 (34.66%)	38a $\pm$ 1.73 (50.66%)	51a $\pm$ 2.08 (68%)	61a $\pm$ 2.30 (81.33%)
	DW	0e $\pm$ 0 (0%)	0e $\pm$ 0 (%)	0e $\pm$ 0 (%)	0e $\pm$ 0 (%)
Degrees of freedom	4	4	4	4	4
Sum of squares	1146	2582.40	4472.40	6561.60	
Mean squares	286.50	645.60	1118.10	1640.40	
F-calculated	53.05	134.50	155.29	174.51	
Significance	0.00000	0.00000	0.00001	0.00002	

<sup>a</sup> Each value is an average of six replicates, DW = double water (control), SE=standard error, J2s-second-stage juveniles, values are given in parentheses represent percent J2s mortality over control, values are given without parentheses represent number of the dead J2s of *M. incognita* in different concentrations of *C. bonplandianus* leaves extract.

processing costs are two examples of issues that may limit the large-scale production of plant extracts. More research is needed to improve extraction methods and investigate the possibility of growing these plants on a big scale to increase viability. Furthermore, combining plant-based nematicides with other methods of controlling pests, including crop rotation or organic soil amendments, may improve their overall effectiveness and financial feasibility in agricultural production. To guarantee uniformity in efficacy under various environmental

circumstances, standardized formulations might also be required.

The nematicidal properties of 4-vinylphenol against *M. incognita* included contact activity, fumigation activity, suppressing egg hatching activity, repellent activity at high concentration, and trapping activity at low concentration.<sup>31,32</sup> Numerous nematicidal volatile organic compounds, including acetaldehyde, dimethyl disulfide, ethylbenzene, 2-butanone,<sup>33</sup> and 4-vinylphenol,<sup>31</sup> were produced by *Virgibacillus dokdonensis* MCCC 1A00493. With an EC50 of roughly  $0.70 \pm 0.64 \mu\text{g mL}^{-1}$

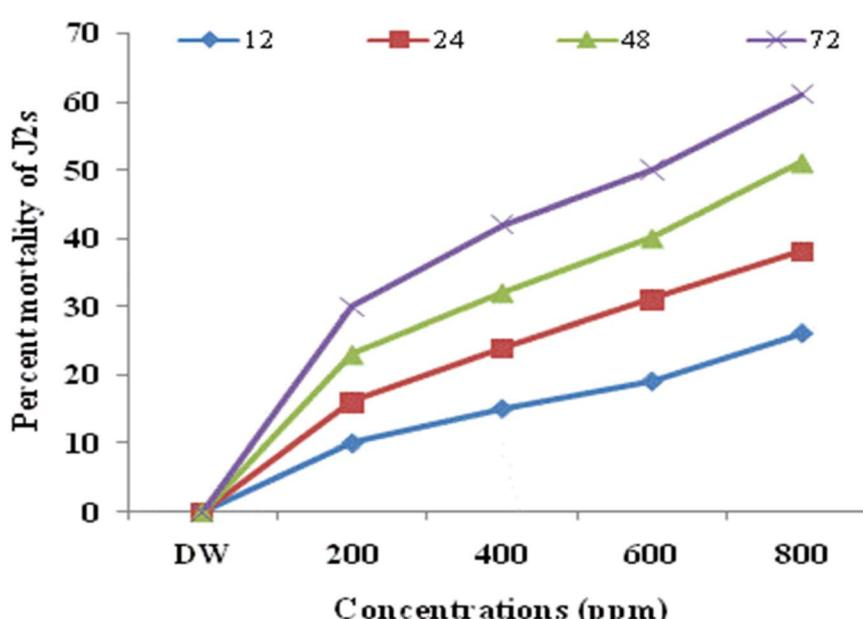


**Fig. 2** Regression lines showing linear relationship between various concentrations of *C. bonplandianus* leaves extract and J2s mortality of *M. incognita*. [DW-distilled water (Control); ppm-parts per million].



**Table 2** Nematicidal activity of *C. bonplandianus* leaves extract against J2s of *M. incognita*<sup>a</sup>

Treatment	Exposure period (hours)	LC50 value in ppm (95% CL)
<i>C. bonplandianus</i>	12	1982.43
	24	834.64
	48	468.46
	72	299.55

<sup>a</sup> LC50 – lethal concentration caused 50% mortality after 12, 24, 48 and 72 h at 95% confidence limits, CL – confidence limit.

following a day of exposure, *p*-nitrophenol was found to have the highest nematicidal activity against *M. incognita*, other compounds such as *m*-nitrophenol, *o*-nitrophenol, and *p*-bromophenol also demonstrated noteworthy effects, with EC50 values of  $8.14 \pm 5.49$ ,  $15.79 \pm 10.81$ , and  $25.92 \pm 11.37 \mu\text{g mL}^{-1}$ , respectively<sup>34</sup>. According to Mondal *et al.*,<sup>35</sup>  $\beta$ -sitosterol-3-O- $\beta$ -D-glucoside, which was isolated from *Mentha spicata*, showed notable nematicidal activity against *M. incognita* after 96 hours, the LC<sub>50</sub> values ranged from 62.64 to 74.19 ppm. At a dose of 100  $\mu\text{g mL}^{-1}$ ,  $\beta$ -sitosterol caused 68.7% immobility after 72 hours, according to another study that examined the effects of stigmasterol and  $\beta$ -sitosterol on *Nacobbus aberrans*.<sup>36</sup> At a dosage of 100 mg  $\text{mL}^{-1}$  over 48 hours, found that  $\beta$ -sitosterol xyloside, which was isolated from the stem bark of *Eucalyptus exserta*, killed 33.6% of *M. incognita*.<sup>37</sup> Infection caused  $\beta$ -sitosterol levels to rise and stigmasterol levels to fall in crops such as corn, soybean, tomato, and cucumber; this change in the  $\beta$ -sitosterol/stigmasterol ratio may be part of the plant's defense mechanisms against nematode invasion.<sup>38</sup>

Phytochemicals released by the breakdown of organic waste are harmful to nematodes that cause root knots.<sup>39</sup> According to a new study by Chin *et al.*,<sup>40</sup> flavonoids are essential for lowering nematode activity because they change their migration patterns toward plant roots, decrease their mobility, repel them, and eventually kill them. Even though more research is required to completely clarify the mechanisms, these chemicals may have nematode nematicidal effects by disrupting nematode cell membranes, interfering with metabolic processes, or reducing reproduction.<sup>40</sup> A key component of integrated pest management (IPM), which ensures food security in response to the growing demand for agricultural production worldwide, is the effective development of biopesticides within sustainable agricultural systems.<sup>41</sup> When tested against *Radopholus similis*, *Pratylenchus penetrans*, and *M. incognita*, different phenolic compounds, alkaloids, and terpenes have shown similar inhibitory effects. In *R. similis* and *M. incognita*, motility and egg hatching are significantly suppressed, but not in *P. penetrans*.<sup>42</sup> According to Kessler *et al.*,<sup>43</sup> volatile chemicals have the ability to both activate resistance-related genes in plants and draw in nematode natural predators. Enhancing plant defense mechanisms to boost the synthesis of nematotoxic secondary metabolites is a viable approach for sustainable nematode management, as evidenced by recent studies and advances in agricultural biotechnology.<sup>44</sup>

### 3.3 GC-MS analysis

The chemical composition and structural properties of different medicinal plant extracts significantly influence their biological potential. The analysis of the methanolic leaf extract of *C. bonplandianus* identified 23 peaks, each representing distinct bioactive compounds. The identification of these compounds was achieved by comparing their retention times and other relevant parameters with reference compounds from the NIST library (Table 3). Fig. 3 illustrates the GC-MS chromatogram of the methanolic extract of *C. bonplandianus*. *In vitro* studies demonstrated that the identified compounds, both individually and in combination, displayed toxic effects on *M. incognita* J2s and egg masses. GC-MS analysis confirmed the presence of metabolically active compounds that contribute to nematicidal activity against *M. incognita*.

Prior research indicates that specific bioactive compounds identified *via* GC-MS exhibit notable biological properties. This technique is essential for chemotaxonomic and active chemical analyses of organic substances that contain physiologically active constituents. The GC-MS analysis of volatile emissions from cotton cake has identified several chemical classes, including terpenes, alcohols, sulfur-containing compounds, ketones, and complex mixtures. The compounds exhibit various applications, notably potential nematicidal effects.<sup>45</sup> The chemotype of *Origanum × Lirium* is largely similar to that of its parent species in terms of both volatile and polar constituents, as evidenced by data from gas chromatography-mass spectrometry (GC-MS) and liquid chromatography-high-resolution mass spectrometry (LC-HRMS) and emphasized by comparative analysis.<sup>46</sup> *Trans*-*p*-(*l*-butenyl)-anisole (1) was identified as a significant constituent of *Wurfbainia schmidii* essential oil, making up 88.69% of the oil, demonstrated virucidal activity against SARS-CoV-2 with an EC50 value of 119.60  $\mu\text{M}$ .<sup>47</sup> By using GC-MS analysis, several frequent chemicals found in *Selaginella bryopteris* were *trans*-13-Octadecenoic acid, methyl ester, eugenol, and hexadecanoic acid.<sup>48</sup> Bioactive compounds 1-octen-3-ol, nonanal, *trans*- $\beta$ -ionone, phytol, *trans*-farnesol, and squalene were identified in *Cucurbita pepo* leaves extract.<sup>49</sup>

### 3.4 Molecular docking analysis

Molecular docking analysis was performed to evaluate the binding affinity and interaction profile of ODR 1 with 4-vinylphenol and gamma-sitosterol. The binding energy of ODR 1 with 4-vinylphenol was found to be  $-5.71 \text{ kcal mol}^{-1}$ , whereas the interaction of ODR 1 with gamma-sitosterol exhibited a significantly higher binding affinity, with a binding energy of  $-12.21 \text{ kcal mol}^{-1}$ . The interaction details for both compounds revealed distinct binding patterns, suggesting differences in molecular recognition and stability of the ligand-protein complexes. In the case of 4-vinylphenol, key interactions were observed with MET84 and MET91, where the benzene ring participated in Pi-Sulfur interactions with distances of 5.81678 Å and 4.13893 Å, respectively (Table 4). Additionally, PHE123 exhibited Pi-Pi T-shaped interactions with the benzene ring at a distance of 5.78983 Å, indicating aromatic stabilization. Alkyl interactions were noted between ALA88, MET91, and TRP114



Table 3 Catalog of detected compounds present in methanolic extract of leaves of *C. bonplandianus* determined by GC-MS technique

Peak number	Retention time	Height	Area	Area%	Name of compound	Molecular formula	Molecular weight (g mol <sup>-1</sup> )
1	12.354	343691	5 156 524	5.43	4H-pyran-4-one,2,3-dihydro-3,5-dihydroxy-6-methyl	C <sub>6</sub> H <sub>8</sub> O <sub>4</sub>	144.12
2	15.153	434202	7 885 574	8.31	4-Vinylphenol	C <sub>8</sub> H <sub>8</sub> O	120.15
3	17.527	338606	2 419 119	2.55	2-Methoxy-4-vinylphenol	C <sub>9</sub> H <sub>10</sub> O <sub>2</sub>	150.17
4	30.313	95981	268017	0.28	Isopropyl myristate	C <sub>17</sub> H <sub>34</sub> O <sub>2</sub>	270.5
5	30.567	615065	1 809 313	1.91	Neophytadiene	C <sub>20</sub> H <sub>38</sub>	278.5
6	31.092	81222	261146	0.28	2-Hexadecen-1-ol,3,7,11,15-tetramethyl	C <sub>20</sub> H <sub>40</sub> O	296.5
7	31.157	177947	566615	0.60	1,2-Benzenedicarboxylicacid,bis(2-methylpropyl) ester	C <sub>16</sub> H <sub>22</sub> O <sub>4</sub>	278.34
8	33.349	678892	2 984 398	3.14	n-Hexadecanoic acid	C <sub>16</sub> H <sub>32</sub> O <sub>2</sub>	256.42
9	35.985	182849	553775	0.58	9,12,15-Octadecatrienoic acid	C <sub>18</sub> H <sub>30</sub> O <sub>2</sub>	278.42
10	36.191	1 125 255	3 951 991	4.16	Phytol	C <sub>20</sub> H <sub>40</sub> O	296.5
11	40.083	185895	756323	0.80	Oxazole	C <sub>3</sub> H <sub>3</sub> NO	69.06
12	42.259	90178	309551	0.33	Cyclohexane	C <sub>6</sub> H <sub>12</sub>	84.16
13	42.472	176748	630413	0.66	3-Cyclopentylpropionic acid	C <sub>8</sub> H <sub>14</sub> O <sub>2</sub>	142.20
14	46.251	98394	291962	0.31	n-Tetracosanol-1	C <sub>24</sub> H <sub>50</sub> O	354.65
15	47.941	1 202 955	3 683 497	3.88	Squalene	C <sub>30</sub> H <sub>50</sub>	410.7
16	49.905	985595	3 613 993	3.81	Delta-tocopherol	C <sub>27</sub> H <sub>46</sub> O <sub>2</sub>	402.7
17	51.129	449731	1 542 308	1.62	Beta-tocopherol	C <sub>28</sub> H <sub>48</sub> O <sub>2</sub>	416.7
18	52.438	9 508 765	35 668 892	37.58	DL-alpha-tocopherol	C <sub>29</sub> H <sub>50</sub> O <sub>2</sub>	430.7
19	53.905	675730	3 145 825	3.31	Ergost-5-en-3-ol	C <sub>28</sub> H <sub>48</sub> O	400.7
20	54.276	219950	926579	0.98	Stigmasterol	C <sub>29</sub> H <sub>48</sub> O	412.7
21	55.222	1 338 060	7 035 915	7.41	Gamma-sitosterol	C <sub>29</sub> H <sub>50</sub> O	414.7
22	55.470	221014	1 245 355	1.31	Fucosterol	C <sub>29</sub> H <sub>48</sub> O	412.7
23	55.979	100798	373829	0.39	Beta-amyrin	C <sub>30</sub> H <sub>50</sub> O	426.7

with the C9 carbon of 4-vinylphenol, suggesting moderate hydrophobic contacts (Fig. 4a and b). These interactions contributed to the stability of the ligand within the binding pocket, though the relatively higher binding energy suggests weaker overall binding compared to gamma-sitosterol.

Conversely, docking of gamma-sitosterol with ODR 1 revealed a much stronger interaction, reflected in a significantly lower binding energy. TRP114 played a crucial role, participating in multiple Pi-Sigma and Pi-alkyl interactions with the C20, C25, C26, and benzene ring of the ligand, suggesting

strong  $\pi$ -electron cloud stabilization. Additionally, LEU73, LEU76, and ALA88 contributed to alkyl interactions, further enhancing hydrophobic contacts (Table 5). The presence of multiple binding interactions across various amino acids, particularly involving TRP114, suggests that gamma-sitosterol achieves a deeper and more stable binding within the active site (Fig. 5a and b).

The comparison between the two docking results highlights a clear difference in binding affinity and interaction strength. Gamma-sitosterol exhibited a much stronger binding affinity

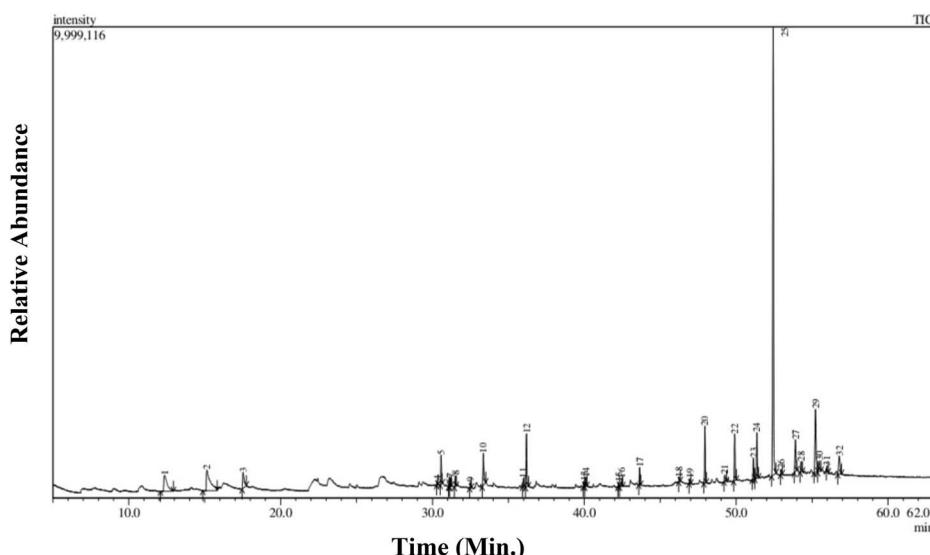


Table 4 Types of bonds involved in the interaction of ODR 1 with 4-vinylphenol

S.N.	Amino acid of ODR-1	Atoms of 4-vinylphenol	Type of interactions involved	Distance (Å)
1	MET84	Benzene ring	Pi-sulfur	5.81678
2	MET91	Benzene ring	Pi-sulfur	4.13893
3	PHE123	Benzene ring	Pi-pi T-shaped	5.78983
4	ALA88	C9	Alkyl	3.81317
5	MET91	C9	Alkyl	4.31468
6	TRP114	C9	Pi-alkyl	3.9399
7	TRP114	C9	Pi-alkyl	4.23234

(−12.21 kcal mol<sup>−1</sup>) than 4-vinylphenol (−5.71 kcal mol<sup>−1</sup>), nearly doubling the binding energy, which suggests a more stable complex formation. The presence of multiple hydrophobic interactions, especially Pi-alkyl interactions with TRP114, likely contributed to the stronger affinity of gamma-sitosterol. In contrast, 4-vinylphenol, being a smaller and less hydrophobic molecule, engaged in fewer stabilizing interactions, leading to a relatively weaker binding.

These findings suggest that gamma-sitosterol is a more potent binder to ODR 1 compared to 4-vinylphenol, which could have implications in its biological role and functional relevance. The strong binding affinity observed for gamma-sitosterol might indicate a higher potential for modulating ODR 1 activity, possibly influencing its role in ligand transport or signal transduction. In contrast, 4-vinylphenol, while still interacting with ODR 1, may have a more transient or less stable

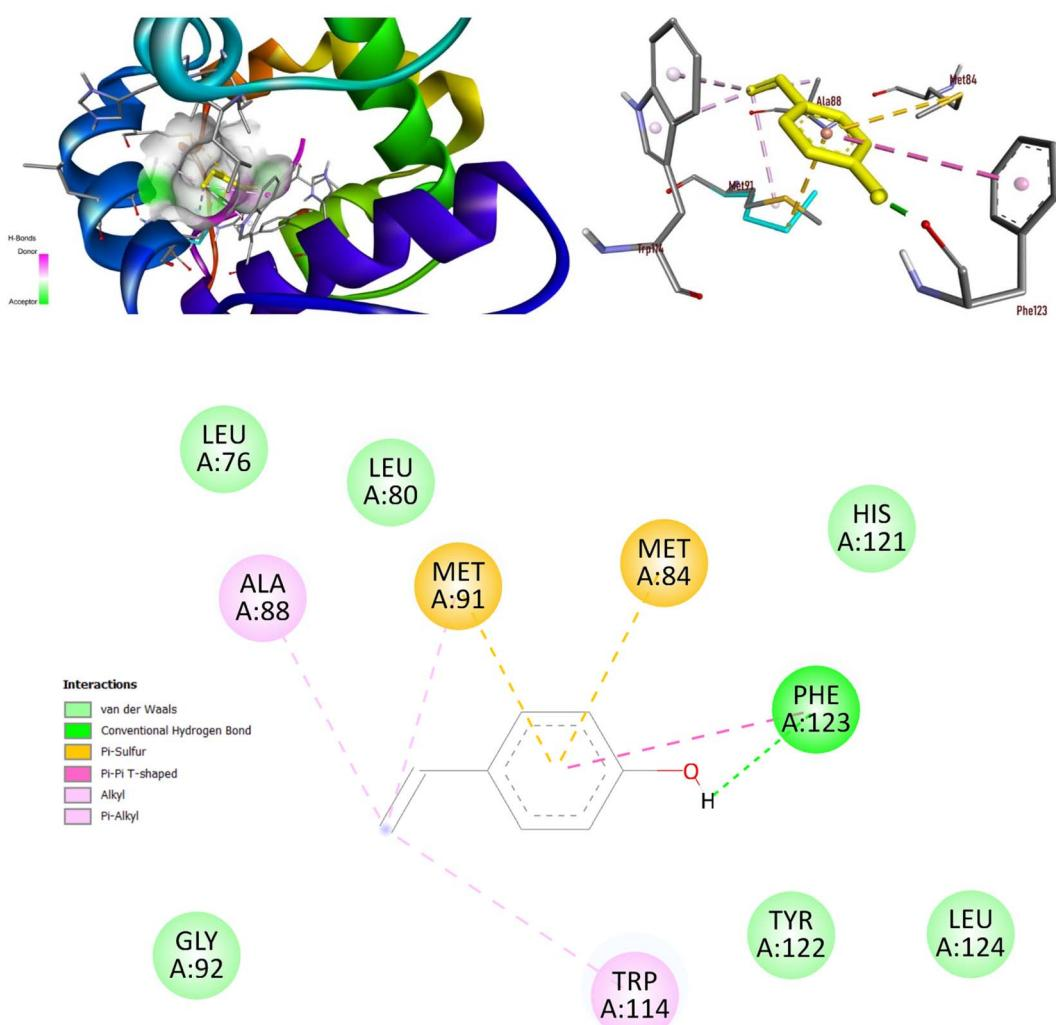


Fig. 4 (a) 3D structure for molecular docking of ODR 1 with 4-vinylphenol. (b) 2D schematic representation for the interaction of ODR 1 with 4-vinylphenol.



Table 5 Types of bonds involved in the interaction of ODR 1 with 4-gamma sitosterol

S.N.	Amino acid of ODR-1	Atoms of 4-gamma sitosterol	Type of interactions involved	Distance (Å)
1	TRP114	C20	Pi-sigma	3.67498
2	TRP114	C25	Pi-sigma	3.96905
3	LEU73	Benzene ring	Alkyl	4.84762
4	LEU73	Benzene ring	Alkyl	5.07228
5	ALA88	Benzene ring	Alkyl	3.81423
6	ALA88	C27	Alkyl	4.47273
7	LEU76	C27	Alkyl	4.59996
8	HIS77	C18	Pi-alkyl	5.1741
9	TRP114	C26	Pi-alkyl	5.1201
10	TRP114	Benzene ring	Pi-alkyl	5.06677
11	TRP114	Benzene ring	Pi-alkyl	4.20402
12	TRP114	C26	Pi-alkyl	4.6844

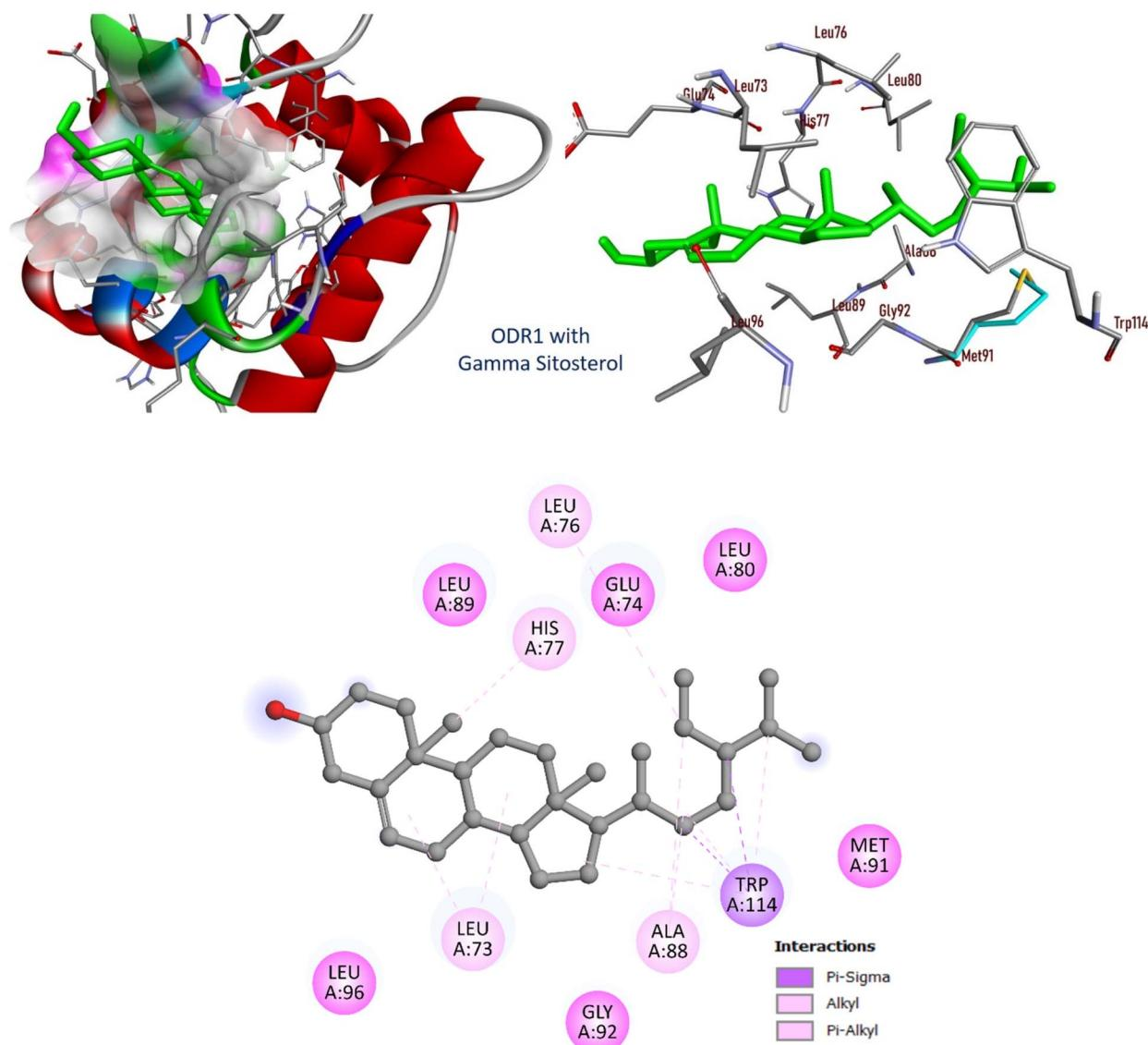


Fig. 5 (a) 3D structure for molecular docking of ODR 1 with gamma-sitosterol. (b) 2D schematic representation for the interaction of ODR 1 with gamma-sitosterol.



interaction, making it a weaker candidate for ODR 1-mediated processes. Overall, the results provide molecular insight into the differential binding behaviors of these two compounds, emphasizing the significance of hydrophobic interactions and ligand size in determining the strength of ligand-protein interactions.

Odorant response gene 1 (odr-1) plays a crucial role in the chemosensory behavior of root-knot nematodes (RKNs) like *Meloidogyne incognita* and *Meloidogyne graminicola*, this gene encodes a membrane-bound guanylyl cyclase involved in the detection of chemical cues essential for host location and infection processes.<sup>50,51</sup> RNA interference (RNAi) studies have demonstrated that silencing Mi-odr-1 (*M. incognita*-ODR 1) leads to behavioral defects, including impaired chemotaxis toward various volatile and non-volatile compounds, as well as reduced attraction to host root exudates, indicates that Mi-odr-1 is essential for effective host-seeking behavior in *M. incognita*.<sup>51</sup> ODR-1 is integral to the chemosensory mechanisms that enable root-knot nematodes to locate and infect host plants, disrupting this gene's function adversely affects their ability to detect chemical cues, thereby reducing their infectivity.<sup>51,52</sup>

## 4. Conclusions

This research evaluates the nematotoxic effects of *C. bonplandianus* leaf extract on *M. incognita* and identifies its metabolic components through GC-MS analysis. *In vitro* studies demonstrated that all identified nano compounds, both individually and in combination, displayed toxicity to *M. incognita*. The leaf extract of *C. bonplandianus* is characterized by a rich composition of bioactive compounds, which are likely responsible for its nematicidal properties, positioning it as a promising candidate for the development of natural nematicides. Plant-based extracts function as alternatives or complementary agents to synthetic nematicides in the management of plant-parasitic nematodes within agricultural systems. Molecular docking approaches offer a systematic method for the selection of natural products and the identification of biopesticide candidates through the elucidation of their bioactivity. In future work, the biologically active compounds in this article also need to be identified and purified before clinical experiments. These are mixtures of various compounds. Distinct biological activities against humans require the use of a pure, identified material. The application of *C. bonplandianus* leaf extract in IPM serves as a safe, cost-effective, and environmentally friendly approach to controlling RKNs. The integration of *C. bonplandianus* leaf extract into agricultural practices has the potential to improve soil physicochemical properties and offer a sustainable, cost-effective approach for managing RKNs.

## Data availability

Data will be made available upon reasonable request from authors.

## Author contributions

AHJ: Writing-original draft, validation, software, methodology, investigation, formal analysis, data curation, conceptualization. FA, IM: Writing-review & editing, validation, methodology, investigation, formal analysis, data curation, conceptualization, resources, AAA: Writing-review & editing, validation, formal analysis. SKA: Writing-review & editing, supervision, conceptualization, validation, methodology.

## Conflicts of interest

The authors declare that they have no known competing financial interests or personal relationships that could have appeared to influence the work reported in this paper.

## Acknowledgements

This article is derived from a research grant funded by the Research, Development, and Innovation Authority (RDIA)-Kingdom of Saudi Arabia-with grant number (12894-JAZZAN-2023-JZU-R-2-1-SE).

## References

- 1 T. K. Dutta and V. Phani, *Front. Plant Sci.*, 2023, **14**, 1143889.
- 2 M. H. Jensen, in *International Symposium on Design and Environmental Control of Tropical and Subtropical Greenhouses*, 2001, vol. 578, pp. 19–25.
- 3 J. T. Jones, A. Haegeman, E. G. J. Danchin, H. S. Gaur, J. Helder, M. G. K. Jones, T. Kikuchi, R. Manzanilla-López, J. E. Palomares-Rius, W. M. L. Wesemael and R. N. Perry, *Mol. Plant Pathol.*, 2013, **14**, 946–961.
- 4 A. Goverse and G. Smart, *Annu. Rev. Phytopathol.*, 2014, **52**, 243–265.
- 5 A. Ahuja and V. S. Somvanshi, *Crop Prot.*, 2021, **147**, 105459.
- 6 P. T. Makunde, S. Dimbi and T. S. Mahere, *J. Entomol. Nematol.*, 2018, **10**, 1–5.
- 7 M. C. Khosa, Z. Dube, D. De Waele and M. S. Daneel, *J. Nematol.*, 2020, **52**, 2–23.
- 8 M. M. Abd-Elgawad, *Plants*, 2021, **10**, 1–16.
- 9 K. Sarri, S. Mourouzidou, N. Ntalli and N. Monokrousos, *Agronomy*, 2024, **14**, 213.
- 10 I. O. Giannakou, *Eur. J. Plant Pathol.*, 2011, **130**, 587–596.
- 11 N. Javed, S. R. Gowen, M. Inam-ul-Haq, K. Abdullah and F. Shahina, *Crop Prot.*, 2007, **26**, 911–916.
- 12 R. Cetintas and M. M. Yarba, *J. Anim. Vet. Adv.*, 2010, **9**, 222–225.
- 13 P. Barbosa, J. M. S. Faria, T. Cavaco, A. C. Figueiredo, M. Mota and C. S. L. Vicente, *Plants*, 2024, **13**, 726.
- 14 R. Ferreira, C. Maleita, L. Fonseca, I. Esteves, I. Sousa-Ferreira, R. Cabrera and P. Castilho, *Plants*, 2025, **14**, 337.
- 15 N. Sivasubramiam, G. Hariharan and M. C. M. Zakeel, in *Management of Phytonematodes: Recent Advances and Future Challenges*, Springer, Singapore, 2020, pp. 353–399.
- 16 D. Tsikas, *J. Clin. Med.*, 2024, **13**, 7276.



17 S. W. Kattan, M. S. Nafie, G. A. Elmgeed, W. Alelwani, M. Badar and M. A. Tantawy, *J. Steroid Biochem. Mol. Biol.*, 2020, **198**, 105604.

18 A. Lee and D. Kim, *Bioinformatics*, 2020, **36**, 959–960.

19 Z. Dutkiewicz and R. Mikstacka, *Int. J. Mol. Sci.*, 2025, **26**, 1002.

20 J. D. Eisenback and D. J. Hunt, in *Root-Knot Nematodes*, ed. J. L. Starr, M. Moens and R. N. Perry, CABI, Wallingford, UK, 2009, pp. 18–54.

21 F. M. Almutairi, A. Khan, M. R. Ajmal, R. H. Khan, M. F. Khan, H. Lal, M. Ullah, F. Ahmad, L. Ahamad, A. Khan, *et al.*, *Life*, 2022, **12**, 2109.

22 K. G. El-Rokiek and W. M. El-Nagdi, *J. Plant Prot. Res.*, 2011, **51**, 121–129.

23 N. Aissani, P. P. Urgeghe, C. Oplos, M. Saba, G. Tocco, G. L. Petretto, K. Eloh, U. Menkissoglu-Spirooudi, N. Ntalli and P. Caboni, *J. Agric. Food Chem.*, 2015, **63**, 6120–6125.

24 M. Sakuma, *Appl. Entomol. Zool.*, 1998, **33**, 339–347.

25 A. S. Behreus and L. Karbeur, *Archiv. Exp. Pathol. Pharmakol.*, 1953, **28**, 177–183.

26 M. Amir, M. A. Qureshi and S. Javed, *J. Biomol. Struct. Dyn.*, 2020, **39**, 3934–3947.

27 M. Amir, M. A. Qureshi, A. Khan, S. M. Nayeem, W. A. Malik and S. Javed, *Spectrochim. Acta, Part A*, 2024, **308**, 123678.

28 M. Amir, F. Nabi, S. M. F. Zaheer, R. H. Khan and S. Javed, *J. Mol. Liq.*, 2024, **401**, 124642.

29 M. Amir and S. Javed, *Int. J. Biol. Macromol.*, 2023, **241**, 124656.

30 O. P. Sheoran, D. S. Tonk, L. S. Kaushik, R. C. Hasija and R. S. Pannu, in *Recent Advances in Information Theory, Statistics & Computer Applications*, ed. D. S. Hoda and R. C. Hasija, Department of Mathematics Statistics, CCS HAU, Hisar, India, 1998, pp. 139–143.

31 D. Huang, H. Yu, W. Chen, W. L. Cheng, Z. Z. Shao and J. B. Zhang, *Acta Microbiol. Sin.*, 2022, **62**, 346–356.

32 W. Chen, Z. Zhu, C. Liu, F. Yang, W. Dai, H. Yu, *et al.*, *Biol. Control*, 2024, **192**, 105508.

33 D. Huang, C. Yu, Z. Shao, M. Cai, G. Li, L. Zheng, Z. Yu and J. Zhang, *Molecules*, 2020, **25**, 744.

34 N. Aissani, R. Balti and H. Sebai, *J. Helminthol.*, 2018, **92**, 668–673.

35 P. C. Mondal, V. Kumar, P. Kaushik, *et al.*, *J. Plant Dis. Prot.*, 2024, **131**, 1983–1992.

36 R. Velasco-Azorsa, H. Cruz-Santiago, I. Cid del Prado-Vera, M. V. Ramirez-Mares, M. D. R. Gutiérrez-Ortiz, N. F. Santos-Sánchez, R. Salas-Coronado, C. Villanueva-Cañongo, K. I. Lira-de León and B. Hernández-Carlos, *Molecules*, 2021, **26**, 2216.

37 J. Li and H. Xu, *Ind. Crops Prod.*, 2012, **40**, 302–306.

38 A. Cabianca, L. Müller, K. Pawłowski and P. Dahlin, *Plants*, 2021, **10**, 292.

39 P. W. Mashela, M. S. Daneel, D. De Waele, H. Fourie, M. C. Khosa, K. M. Pofu and G. M. Tefu, in *Nematology in South Africa: A View from the 21st Century*, ed. H. Fourie, V. W. Spaull, R. Jones, M. S. Daneel and D. De Waele, Springer, Cham, Switzerland, 2017, pp. 151–181.

40 S. Chin, C. A. Behm and U. Mathesius, *Plants*, 2018, **7**, 85.

41 Food and Agriculture Organization of the United Nations, <https://www.fao.org/documents/card/en?details=cc7724en>, (accessed January 4, 2024).

42 N. Wuyts, R. Swennen and D. De Waele, *Nematology*, 2006, **8**, 89–101.

43 A. Kessler, R. Halitschke, C. Diezel and I. T. Baldwin, *Oecologia*, 2006, **148**, 280–292.

44 K. Sato, Y. Kadota and K. Shirasu, *Front. Plant Sci.*, 2019, **10**, 1165.

45 T. S. A. Monteiro, É. D. G. C. Nasu, C. P. Guimarães, W. D. S. Neves, E. H. Mizobutsi and L. G. D. Freitas, *Cienc. Rural*, 2014, **44**, 1149–1154.

46 E. A. Petrakis, E. V. Mikropoulou, S. Mitakou, M. Halabalaki and E. Kalpoutzakis, *Phytochem. Anal.*, 2023, **34**, 289–300.

47 C. Sagayap, P. Chuysinuan, N. Chutiwittonchai, P. Pripdeevech, W. Kaewsri, S. Sureram, N. Chantratita, K. Lirdprapamongkol, J. Svasti, S. Techasakul and C. Mahidol, *Nat. Prod. Commun.*, 2025, **20**, 1–10.

48 U. Srivastava and A. Mathur, *Data Brief*, 2025, **59**, 111318.

49 E. I. Akubugwo, O. Emmanuel, C. N. Ekweogu, O. C. Ugbogu, T. R. Onuorah, O. G. Egeduzu and E. A. Ugbogu, *Sci. Pharm.*, 2022, **90**, 64.

50 T. K. Dutta, V. S. Akhil, M. Dash, A. Kundu, V. Phani and A. Sirohi, *BMC Genomics*, 2023, **24**, 745.

51 T. N. Shivakumara, T. K. Dutta, S. Chaudhary, S. H. von Reuss, V. M. Williamson and U. Rao, *Mol. Plant-Microbe Interact.*, 2019, **32**, 876–887.

52 T. K. Dutta, V. S. Akhil, A. Kundu, M. Dash, V. Phani, A. Sirohi and V. S. Somvanshi, *Heliyon*, 2024, **10**, e26384.

